MJFAS Malaysian Journal of Fundamental and Applied Sciences
ISSN:2289-5981 e-ISSN:2289-599X
UTM UNIVERSITI TEKNOLOGI MALAYSIA

# Photoisomerization of *n*-pentane over nano ZnO/$MoO_3$-$ZrO_2$

Sugeng Triwahyono[1,2*], Aishah Abdul Jalil[3,4] and Che Rozid Mamat[2]

[1]*Ibnu Sina Institute for Fundamental Science Studies, Universiti Teknologi Malaysia, 81310 UTM Johor Bahru, Johor, Malaysia*
[2]*Department of Chemistry, Faculty of Science, Universiti Teknologi Malaysia, 81310 UTM Johor Bahru, Johor, Malaysia*
[3]*Department of Chemical Eng., Faculty of Chemical Eng., Universiti Teknologi Malaysia, 81310 UTM Johor Bahru, Johor, Malaysia*
[4]*Institute Hydrogen Economy, Universiti Teknologi Malaysia, 81310 UTM Johor Bahru, Johor, Malaysia*
**Corresponding Author: sugeng@utm.my (S. Triwahyono)*

***Article history :***
*Received 22 March 2014*
*Revised 17 June 2014*
*Accepted 21 July 2014*
*Available online 18 August 2014*

**GRAPHICAL ABSTRACT**

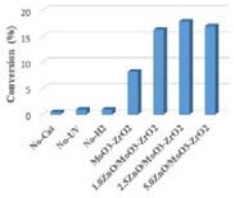


**ABSTRACT**

A series of nano ZnO/$MoO_3$-$ZrO_2$ catalysts with different ZnO loading (1.0, 2.5, 5.0 wt%) were prepared by impregnation method for *n*-pentane photoisomerization under hydrogen or nitrogen atmosphere. The properties of the catalysts were characterized with X-ray Diffraction (XRD), Brunauer Emmett Teller (BET), Transmission Electron microscope (TEM) and FTIR. The XRD result showed that the fraction of tetragonal phase of ZnO/$MoO_3$-$ZrO_2$ was about 0.67 for all samples. While, the specific BET surface area was about 24 $m^2$/g. Pyridine adsorbed FTIR results showed that all samples possessed high concentration of strong Lewis acid sites and small concentration of weak Bronsted acid sites. The interaction of hydrogen and surface samples at 298-523 K formed protonic acid sites with the concomitant of the partial elimination of Lewis acid sites. Whereas no changes of the concentration of acid sites were observed in the presence of nitrogen atmosphere. The activity of all samples in the n-pentane photoisomerization was strongly determined by the presence of hydrogen gas. In fact no activity was observed in the absence of hydrogen.

*Keywords: ZnO/$MoO_3$-$ZrO_2$, nano ZnO, protonic acid sites, n-pentane photoisomerization*


http://dx.doi.org/10.11113.mjfas.v10n4.320

## 1. INTRODUCTION

The operation of a modern refinery nowadays is becoming more and more complicated. World-wide public are now having a great concerns about the earth's environment and health considerations led into several new legislative actions around the world. With the demand to meet clean fuels challenge the processing configuration has to be adapted accordingly. Since the launching of unleaded gasoline in the USA in the early 1970s, environmental issues have dominated the refining planning decisions. Focusing on gasoline, several trends could be identified.

Germany has launched 10 ppm wt. sulphur premium fuels by 2003 through tax incentives while the MTBE phase-out is being banned in the US where leakage of the underground storage tanks have caused pollution of ground water sources. Thus, oil refiners have to seek ways to manage the theoretical octane reduction in the gasoline pool. Furthermore, managing the toxic benzene content in the gasoline pool in addition to the MTBE problem has also become a crucial issue [1-3].

In this regard, isomerization of light straight-run naphtha perfectly fits the processing so called reformulated gasoline. In this context, naphtha-isomerization is of particular interest as it can be established in a refinery at low investment, using idle reactors from either hydroprocessing or catalytic reforming. Besides, modern isomerization technology has contributed to a number of other substantial advantages to the refiner. Traditionally, users of paraffin isomerization technology had to choose either robust zeolite based catalysts or chlorided alumina based systems [4,5]. While zeolite catalysts are characterized by their excellent tolerance of feedstock poisons such as sulphur and water [6-8].

A few years ago metal oxide based isomerization catalysts were launched to the market which not live up to expectations in terms of feedstock tolerance and robustness so that existing metal oxide catalysts are closer to chlorinated catalysts as concerns water sensitivity. A zirconia-based catalyst is distinguished by outstanding activity along with greatly advanced tolerance towards water [9-13]. Together with the excellent sulphur resistance, this catalyst can be used for a variety of feedstocks without expensive pretreating of feedstocks. The octane gain over zeolitic catalysts is in the range of 2–3 RON points, depending on the feedstock composition; hence the activity is closer to chlorinated catalysts than zeolite catalysts.

The studies of solid acid based catalyst have been increasing extensively for the textural, structural and catalytic properties as well as the catalytic behavior of mixed oxide catalyst. $ZrO_2$ is attracting a big interest of its potential as a catalyst support. Zirconia-based solid acid catalyst has become an efficient catalyst for isomerization of alkane. Particularly, Mo/$ZrO_2$ catalysts are better than other classical catalyst due to their acidic properties. The specific activity of molybdenum at low surface

concentration on zirconia was found to be significant higher than alumina or silica. Thus, if Mo can be dispersed at surface of zirconia sufficiently, then a more active catalyst could be synthesized. In addition, the addition of nano-ZnO which has high phototocatalytic activity will provide a new interesting research area of photoisomerization of alkane [14,15]. Nanosized ZnO was recently recognized to be comparable with TiO2 and has received much attention because of its unique properties and numerous advantages. The combination of solid acid catalyst and photocatalyst for isomerization of n-pentane at room temperature will be an interesting process in general catalysis.

## 2. EXPERIMENTAL

### 2.1 Preparation of $MoO_3$-$ZrO_2$ Catalyst

$Zr(OH)_4$ was prepared from zirconium oxychloride by hydrolysis with dilute aqueous ammonia solution. $ZrOCl_2 \cdot 8H_2O$ was dissolved in double distilled water and aqueous $NH_3$ has been added dropwisely into the solution under vigorous stirring until the pH of 8, then the product was washed with hot-distilled water and dried at 393 K overnight [16]. Ammonium heptamolybdate complex was prepared by dissolving of $MoO_3$ in ammonium hydroxide and stirred vigorously for overnight at 353-363 K. Then 5 wt% $MoO_3$-$ZrO_2$ was prepared by impregnation of $Zr(OH)_4$ with ammonium heptamolybdate solution at 353 K. The product then was dried at 383 K overnight, followed by calcination at 1093 K for 3 h.

### 2.2 Preparation of Nano ZnO/$MoO_3$-$ZrO_2$ Catalyst

$Zn^{2+}$ was obtained by anodic oxidation of zinc through a simple electrolysis process which employed a mixture of naphthalene, tetraethylammonium perchlorate (TEAP) and *N,N*-dimethlyformamide (DMF) as electrolyte [17]. The electrolysis was performed at 135 mA for 3 h to produce about 52 g of metal solution that contain 0.67 g of ion $Zn^{2+}$. Nano ZnO/$MoO_3$-$ZrO_2$ was prepared by impregnation of 5wt% $MoO_3$-$ZrO_2$ with 1.0, 2.5 and 5.0 wt% of ZnO. The products were left overnight and followed by drying at 383 K overnight, followed by calcination at 823 K for 3 h.

### 2.3 Characterization of the glass-ceramics

The crystalline structure of the catalyst was determined with X-ray diffraction (XRD) recorded on a powder diffractometer (Bruker Advance D8, 40 kV, 40 mA) using a Cu Kα radiation source in the range of $2\theta = 1.5$-90°. The BET analysis of the catalyst was determined by $N_2$ adsorption-desorption isotherms using a Quantachrome Autosorb-1 instrument. The catalyst was outgassed at 573 K for 3 h before being subjected to $N_2$ adsorption.

DRUV-visible absorption spectra were recorded using UV-Vis Diffuse Reflectance (Perkin-Elmer Lambda 900 spectrometer). The scanning wavelength range was 300-500 nm. In the FTIR measurements, pyridine has been used as a probe molecule for the characterization of acidic sites. All the measurements were performed on an Agilent Cary 640 FTIR spectrometer equipped with a high-temperature stainless steel cell with $CaF_2$ windows. Prior to the measurements, 30 mg of sample in the form of a self-supported wafer was reduced in $H_2$ stream (100 ml/min) at 573 K for 3 h and cooling to 423 K under He atmosphere. For pyridine adsorption, the reduced catalyst was exposed to 2 Torr of pyridine at 423 K for 30 min, followed by outgassing at 523 and 573 K for 30 min, respectively. All spectra were recorded at room temperature with a spectral resolution of 5 $cm^{-1}$ with five scans.

The adsorption and desorption of $H_2$ was done by exposing of pyridine preadsorbed sample with 150 Torr $H_2$ at room temperature followed by heating from 298 to 523 K and outgassing from 323 to 573 K.

### 2.4 Photoisomerization of *n*-pentane

The photoisomerization of *n*-pentane was performed under hydrogen or nitrogen atmosphere in a microcatalytic pulse reactor equipped with UV lamp (4x9W; 365 emission) according to the method described in the literature [14]. Prior to the reaction, 0.2 g of catalyst was placed in quartz glass reactor and was heat-treated in a flow of oxygen ($F_{Oxygen}$=100 ml/min) for 1 h, followed by hydrogen ($F_{Hydrogen}$=100 ml/min) for 3 h at 673 K and cooled down to room temperature in a hydrogen stream. A dose of *n*-pentane (43 µmol) was injected over the activated catalyst under UV irradiation and hydrogen or nitrogen stream, and the products were trapped at 77 K before flash-evaporation into an online 6090N Agilent gas chromatograph equipped with HP-5 Capillary Column and FID detector. The intervals between each pulse injection were kept constant at 20 min.

## 3. RESULTS & DISCUSSION

### 3.1 ZnO nanoparticle

Fig. 1 shows the XRD pattern of ZnO nanoparticles obtained from the electrolysis. The relatively high intensity of peaks showed that the ZnO was in the high crystalline form of ZnO. All peaks are well-matched with the typical single crystalline wurtzite hexagonal phase bulk ZnO (JCPDS file No. 36-1451). Fig. 2 shows the TEM and HRTEM images of ZnO nanoparticle in which the size of ZnO was approximately in the range of 4-9 nm. The specific BET surface area was about 60 $m^2/g$.

Fig. 3 depicts the typical DRUV–vis spectrum of the ZnO at room temperature. A broad band can be seen at 366 nm (3.35 eV), which is very close to the band gap of the ZnO 1s–1s electron transition (3.37 eV) [14]. Thus, this result indicates that the prepared ZnO nanoparticles absorb visible-light as well as ultraviolet-light [18]. Therefore, ZnO nanoparticles are predicted to be good alternatives for visible-light and/or UV photocatalysis materials.

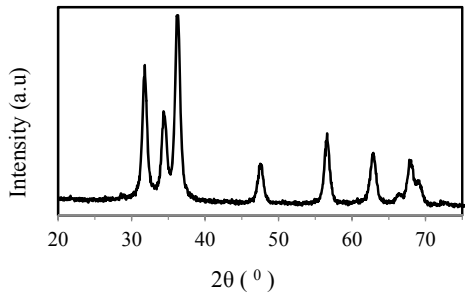


**Fig. 1** X-ray Diffraction pattern for ZnO

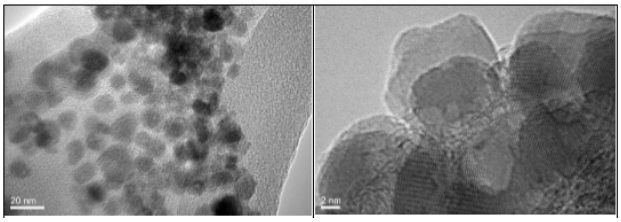

**Fig. 2** TEM images for ZnO

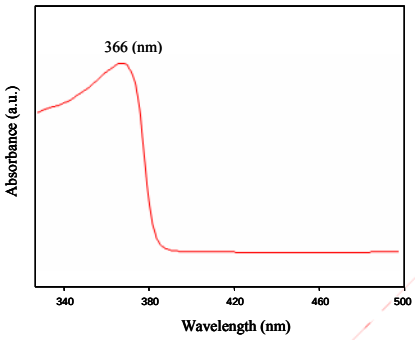


**Fig. 3** DRUV–visible spectrum of ZnO at room temperature

### 3.2 Nano ZnO/$MoO_3$-$ZrO_2$

The diffractograms of XRD in Fig. 4 show peaks at the range of 2θ = 28-29°, 30-31° and 31-32° which correspond to presence of monoclinic and tetragonal phases of $ZrO_2$. The loading of ZnO on $MoO_3$-$ZrO_2$ did not change much the peak position and intensity showing that the nano ZnO did not interact strongly with $MoO_3$-$ZrO_2$. The volumetric ratio of monoclinic to tetragonal was about 30/70. Compared to $MoO_3$-$ZrO_2$, tetragonal phase of different loading ZnO/$MoO_3$-$ZrO_2$ is slightly lower. This indicates that the presence of nano ZnO slightly suppressed the tetragonal phase of zirconia.

The specific BET surface area results showed that 1.0ZnO/$MoO_3$-$ZrO_2$ has a surface area of 24 $m^2$/g. 2.5ZnO/$MoO_3$-$ZrO_2$ has the highest surface area of 26 $m^2$/g while 5.0ZnO/$MoO_3$-$ZrO_2$ has the lowest surface area of 23 $m^2$/g. The introduction of small amount of higher surface area of ZnO did not altered much the surface area of catalysts.

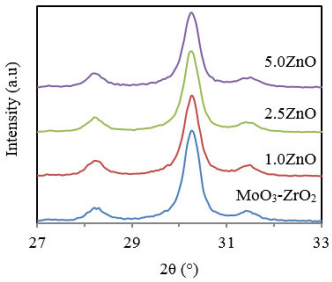


**Fig. 4** X-ray Diffraction pattern for different loading of ZnO

Fig. 5(A) shows the pyridine adsorbed IR spectra for all samples outgassing of pyridine at 523 K and 573 K. For all samples, the intensity of Lewis acid sites at 1450 $cm^{-1}$ decreased slightly as the temperature of outgassing of pyridine increased from 523 to 573 K. This indicated that all samples possess strong Lewis acid sites and small number of weak Lewis acid sites which pyridine molecules were desorbed at and below 573 K. While, only small number of protonic acid sites at 1570 $cm^{-1}$ was observed for all samples. We have reported the acidic study of $MoO_3$-$ZrO_2$ in which the addition of $MoO_3$ on $ZrO_2$ developed strong Lewis and protonic acid sites [19]. Although the addition of nano ZnO did not collapse the crystalline structure and specific surface area of catalyst, the nano ZnO may be interacted with acidic hydroxyl groups in the surface of catalyst which lead to diminishing of the number protonic acid sites on the surface of ZnO/$MoO_3$-$ZrO_2$.

Fig. 5(B) and 5(C) show the changes of IR spectra in the range of 1400-1600 $cm^{-1}$ when the pyridine pre-adsorbed 2.5ZnO/$MoO_3$-$ZrO_2$ sample was heated in the presence of hydrogen up to 523 K followed by heating in vacuum from 323 to 573 K. As shown in Figure 5(B), the intensity of the band at 1450 $cm^{-1}$ decreased slightly and the band at 1570 $cm^{-1}$ increased slightly showing the conversion of Lewis to protonic acid sites. In outgassing process, the intensity of the band at 1450 $cm^{-1}$ increased when the sample was heated from 323 to 573 K in vacuum. While, the intensity of the band at 1570 $cm^{-1}$ restored to almost its original intensity. This indicated that the interchange of Lewis and protonic acid sites in contact and removal of molecular hydrogen at temperature range of 298-573 K. The ability to form protonic acid sites from molecular hydrogen lead to utilize the catalysts in the acid catalytic reaction.

### 3.3 Photoisomerization of *n*-pentane

Fig. 6 show the activity of catalyst in *n*-pentane photoisomerization with the presence and absence of hydrogen. Almost no activity was observed for reactions without catalyst, hydrogen and also UV lamp. The conversion of *n-pentane* did not exceed 2%. The low activity is may be due the absence of ZnO as a photocatalyst agent, the absence of hydrogen as a source of radical H for initiating the isomerization process and the absence of

energy source of ultra violet. The activity increased to about 8% of conversion over $MoO_3$-$ZrO_2$ in the presence of hydrogen and UV irradiation. This result strongly evidenced the necessity of hydrogen, UV irradiation and may be Mo metal which accelerate the formation of isopentane. The addition of nano ZnO increased markedly the conversion of *n*-pentane to about 16, 18 and 17 for 1.0, 2.5 and 5.0 wt% ZnO loaded on $MoO_3$-$ZrO_2$. The presence of ZnO acted as specific active sites for photocatalyst to convert *n*-pentane to isopentane. No by-product were detected in the outlet. Although the reaction mechanism of photoisomerization of *n*-pentane over ZnO/$MoO_3$-$ZrO_2$ is not clear yet, the presence of hydrogen, UV irradiation and nano ZnO determined significantly in the conversion of *n*-pentane to isopentane. In addition the amount of ZnO did not affect significantly in the conversion rate of *n*-pentane.

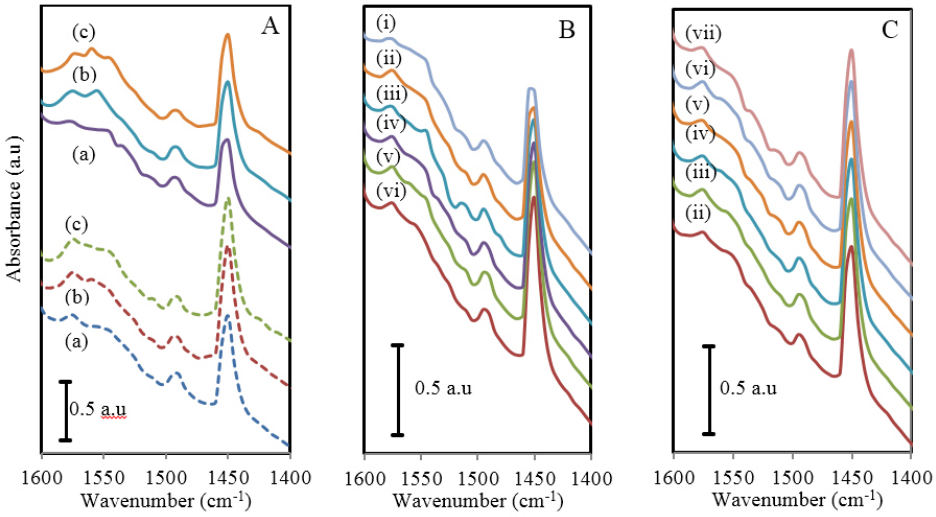


**Fig. 5** (A) Pyridine adsorbed IR spectra of (a) 1.0 ZnO/$MoO_3$-$ZrO_2$, 2.5ZnO/$MoO_3$-$ZrO_2$ and 5.0ZnO/$MoO_3$-$ZrO_2$ at treatment of 523 K (dashed lines) and 573 K (solid lines), Hydrogen (B) adsorption and (C) desorption spectra of 2.5ZnO/$MoO_3$-$ZrO_2$ at (i) 298K, (ii) 298 K, (iii) 323 K, (iv) 423 K, (v)473 K, (vi) 523 K and (vii) 573 K

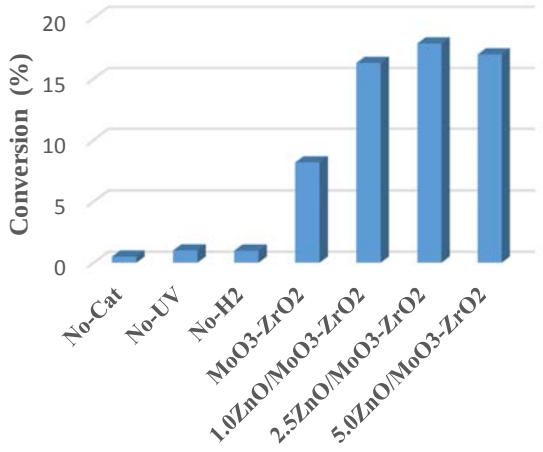


**Fig. 6** Photoisomerization of n-pentane over ZnO/$MoO_3$-$ZrO_2$

## 4. CONCLUSION

Nano ZnO/$MoO_3$-$ZrO_2$ was prepared through impregnation of $Zn^{2+}$ metal solution with $MoO_3$-$ZrO_2$. While, $MoO_3$-$ZrO_2$ can be prepared through impregnation of $Zr(OH)_4$ with $(NH_4)_6Mo_7O_{24}$ complex solution. The nanosized $Zn^{2+}$ metal solution can be prepared by anodic oxidation of zinc through a simple electrolysis process. XRD results showed that the tetragonal phase of $ZrO_2$ did not alter significantly. However, the IR pyridine results showed the absence of protonic acid sites indicating that the nano ZnO interacts with acidic OH groups in the surface of $MoO_3$-$ZrO_2$. Similar to the $MoO_3$-$ZrO_2$, the addition of nano ZnO did not alter the ability of catalyst to form protonic acid sites from molecular hydrogen which is showing the potential of the catalysts to be used in the acid catalytic reaction.

The isomerization of n-pentane has been done under UV irradiation at room temperature in which the results showed the necessity of ZnO, UV irradiation and molecular hydrogen in the formation isopentane. About 17% of *n*-pentane conversion was observed for all ZnO/$MoO_3$-$ZrO_2$ catalyst with the selectivity of isopentane was about 100%.

## ACKNOWLEDGEMENT

This work was supported by Ministry of Higher Education, Malaysia through Fundamental Research Grant no. 4F161, and the Hitachi Scholarship Foundation for the Gas Chromatograph Instruments Grant.

## REFERENCES

[1] H. Weyda, and E. Kohler, Catal. Today, 81 (2003) 51.
[2] A.A Il'icheva, A.Y Olenin, L.I. Podzorova, V.A. Shevchenko,

V.B. Lazarev, A.D. Izotov, Inorg. Mater. 32(7) (1996) 736.
[3] C. Morterra, G. Meligrana, G. Cerrato, V. Solinas, E. Rombi, M.F. Sini, Langmuir19 (2003) 5344.
[4] Keogh R A, Srinivasan R, Davis B H. J Catal, 151(2) (1995) 292.
[5] Farcasiu D, Qi Li J, Kogelbauer A. J Mol Catal A: Chem, 124(1) (1997) 67.
[6] H.D. Setiabudi, A.A. Jalil, S. Triwahyono, J. Catal. 294 (2012) 128.
[7] M. Arif A. Aziz, N. H. Nazirah Kamarudin, Herma Dina Setiabudi, Halimaton Hamdan, Aishah Abdul Jalil, Sugeng Triwahyono, J Nat. Gas Chem. 21 (2012) 29.
[8] N.H.N Kamarudin, A.A. Jalil, S. Triwahyono, R.R. Mukti, M.A.A. Aziz, H.D. Setiabudi, M.N.M.Muhid, H.Halimaton, Appl. Catal A: Gen. 431–432 (2012) 104.
[9] N.H.R. Annuar, A.A. Jalil, S. Triwahyono, Z. Ramli, J Mol. Catal. A: Chem. 377 (2013) 162.
[10] J.C. Yori, C.L. Pieck, J.M. Parera, Catal. Lett. 64 (2000) 141.
[11] S. Triwahyono, T. Yamada, H. Hattori, Appl. Catal. A: Gen. 242 (2003) 101.
[12] S. Triwahyono, T. Yamada, H. Hattori, Catal. Lett., 85 (2003) 109
[13] N.N. Ruslan, N.A. Fadzlillah , A.H. Karim, A.A. Jalil, S. Triwahyono, Appl. Catal. A: Gen. 406 (2011) 102.
[14] N.W.C. Jusoh, A.A. Jalil, S. Triwahyono, H.D. Setiabudi, N. Sapawe, M.A.H. Satar, A.H. Karim, N.H.N. Kamarudin, R. Jusoh, N.F. Jaafar, N. Salamun, J. Efendi, Appl.Catal. A: Gen. 468 (2013) 276.
[15] A.A. Jalil, S. Triwahyono, N.H.H. Hairom, N.A.M. Razali, Mal. J Fund. Appl. Sci. 10(3) (2014) 165.
[16] N.N. Ruslan, S. Triwahyono, A.A. Jalil, S.N. Timmiati, N.H.R. Annuar, Appl. Catal. A: Gen. 413 (2012) 176
[17] N. Sapawe, A.A. Jalil, S. Triwahyono, Mal. J Fund. Appl. Sci. 9(2) (2013) 67.
[18] L. Wu, Y. Wu, W. LÜ, Physica. E 28 (2005) 76.
[19] S. Triwahyono, A.A. Jalil, N.N. Ruslan, H.D. Setiabudi, N.H.N. Kamarudin, J Catal. 303 (2013) 50.